High-Energy Band Structure of Al†

V. Hoffstein* and D. S. Boudreaux‡
Department of Physics, Polytechnic Institute of Brooklyn, Brooklyn, New York 11201
(Received 22 May 1970)

Results of calculating the band structure of metallic Al in the energy range between 0 and 11 Ry, using a pseudopotential method are described. The pseudopotential is similar to that used by Harrison, with several modifications, such as different treatment of conduction-core electron exchange and keeping the full nonlocality of the pseudopotential throughout all calculations. The results were obtained for Δ, Λ, and Σ directions of the fcc lattice. The relative degree of convergence in our calculations varies from 0.02 Ry for the lowest-lying band to 0.2 Ry at about 10 Ry. At the low-energy end (i.e., near the Fermi energy) our results are in good agreement with the previously published data.

I. INTRODUCTION

The electronic band structure and the Fermi surface of Al has been a subject of numerous investigations beginning with that of Heine, [1] who performed the calculation using the orthogonalized-plane-wave (OPW) method. Since then the band structure and the Fermi surface of Al have been calculated by Harrison[2-5] using a pseudopotential method, by Segall[6] using Green's-function method, by Snow[7] who performed a self-consistent calculation using an augmented-plane-wave (APW) method, and by Connolly[8] using an APW method with the potential calculated by Snow. All of the previous investigations (except Connolly's) were concerned with a very narrow energy range – within about 15 eV from the bottom of the first band. This, of course, is entirely sufficient for calculating the topology of the Fermi surface and most of the electronic properties of crystals. There is, however, a variety of problems [e.g., low-energy electron diffraction (LEED) intensities, soft x-ray emission, etc.], which require the knowledge of the excited states at much higher energies – up to 200 eV. The present calculation was in fact motivated by the desire to obtain an elastic LEED spectrum for Al.

II. POTENTIAL, PSEUDOPOTENTIAL, AND METHOD OF CALCULATION

We have adopted an OPW based pseudopotential derived by Harrison[1]; its matrix elements may be written in a slightly more generalized form as

$$\langle \vec{k}+\vec{q}_1 | W | \vec{k}+\vec{q}_2 \rangle = \langle \vec{k}+\vec{q}_1 | V | \vec{k}+q_2 \rangle$$

$$\times \sum_\alpha \left(\frac{h^2}{2m} |\vec{k}+\vec{q}_2|^2 + \langle \vec{k} | V | \vec{k} \rangle - E_\alpha \right]$$

$$\times \frac{\langle \vec{k}+\vec{q}_1 | \alpha \rangle \langle \alpha | \vec{k}+\vec{q}_2 \rangle + (\langle \vec{k}+\vec{q}_1 | P | \vec{k}+\vec{q}_2 \rangle)}{(1 - \langle \vec{k} | P | \vec{k} \rangle)} \Bigg)$$

$$\times \sum_\alpha [(\hbar^2/2m) |\vec{k}|^2 + \langle \vec{k} | V | \vec{k} \rangle - E_\alpha] \langle \vec{k} | \alpha \rangle \langle \alpha | \vec{k} \rangle \ ,$$

$|\vec{k}+\vec{q}\rangle$ is a plane-wave state $\Omega^{-1/2} e^{i(\vec{k}+\vec{q})\cdot\vec{r}}$; $|\alpha\rangle$ is a core state; P is a projection operator onto core states $\sum_\alpha |\alpha\rangle\langle\alpha|$; and V is the crystal potential.

The core functions were taken from the atomic Hartree-Fock calculation by Froese-Fisher.[9] Contributions to the crystal potential V include all of those discussed by Harrison[2]; we differ, however, in the treatment of conduction core-electron exchange. Conventional band-structure calculations all include the exchange potential in the Slater's $\rho^{1/3}$ approximation[2] – primarily because of its computational simplicity. It has now been demonstrated by several workers[10,11] that Slater's approximation may not be adequate in solid state calculations, e.g., Pendry[10] finds that Slater's approximation underestimates the exchange, particularly for large values of $\vec{q}$. Kmetko[11] has investigated the applicability of Slater's exchange for a large number of metals and concluded that if one wants to use a local approximation for the exchange, it must be written as

$$\alpha v_{\text{exch}}^{\text{Slater}}(r),$$

where α is a coefficient which varies from 0.690 to 0.820. In our case, since the pseudopotential is already nonlocal and $\vec{k}$ dependent, a more exact treatment of the exchange does not constitute any major computational difficulties. We have included the exchange between conduction and core electrons in a "single OPW approximation." In this procedure we start with the exact Hartree-Fock exchange operator, assume that a conduction electron is described by a single OPW and take the appropriate munerical core wave functions from Ref. 9. In other words, we have

$$v_i^{\text{exch}}(\vec{r}_1) = -\sum_{nlm} \psi_{nlm}(\vec{r}_1) \int \psi_{nlm}^*(\vec{r}_2) \frac{2}{|\vec{r}_{12}|} \frac{\psi_i(\vec{r}_2) d\vec{r}_2}{\psi_i(\vec{r}_1)} \ .$$

This represents the exchange potential between an electron in state $\psi_i(\vec{r}_1)$ and the core electrons. We assume that the incident electron is described by a single OPW

$$\psi_i(\vec{r}_1) = e^{i\vec{k}\cdot\vec{r}_1} - \sum_{nlm} A_{nlm}(\vec{k})\psi_{nlm}(\vec{r}_1) ,$$

$$A_{nlm}(\vec{k}) = \int \psi^*_{nlm}(\vec{r}')e^{i\vec{k}\cdot\vec{r}'}d\tau' ,$$

$$\psi_{nlm}(\vec{r}) = (1/r)P_{nl}(r)Y_l^m(\theta,\varphi) ,$$

and the summation over nlm means summing over all core-electron states whose spin is the same as that of the conduction electron. This calculation is now carried out in a straightforward manner, making use of the following expansions:

$$\frac{1}{|\vec{r}-\vec{r}'|} = \sum_{l=0}^{\infty}\sum_{m=-l}^{+l}\frac{4}{2l+1}\frac{r_<^l}{r_>^{l+1}}Y_l^{m*}(\Omega')Y_l^m(\Omega) ,$$

$$e^{i\vec{k}\cdot\vec{r}} = \sum_{l=0}[4\pi 2l(2l+1)]^{1/2}\, i^l j_l(kr)Y_l^0(\theta,\varphi) ,$$

and the orthogonality theorem for spherical harmonics. Finally, averaging over the angles, we obtain

$$v^{\text{exch}}(r_1) = -\left[2\frac{P_{10}(r_1)}{r_1}\int rP_{10}(r)\frac{1}{r_>}j_0(kr)\,dr + 2\sqrt{3}\,\frac{P_{21}(r_1)}{r_1}\int rP_{21}(r)\frac{r_<}{r_>^2}j_0(kr)\,dr + \frac{A_{100}}{\sqrt{\pi}}\left(\frac{P_{10}(r_1)}{r_1}\int\frac{1}{r_>}P_{10}^2(r)\,dr\right.\right.$$

$$\left. + \frac{P_{20}(r_1)}{r_1}\int\frac{1}{r_>}P_{20}(r)P_{10}(r)\,dr + \frac{P_{21}(r_1)}{r_1}\int\frac{r_<}{r_>^2}P_{21}(r)P_{10}(r)\,dr\right)$$

$$\left. + \frac{P_{21}(r_1)}{r_1}\int\frac{r_<}{r_>^2}P_{21}(r)P_{20}(r)\,dr\right]\left[\frac{\sin(kr_1)}{kr_1} - \frac{1}{(\sqrt{4\pi})}\left(A_{100}\frac{P_{10}(r_1)}{r_1} + A_{200}\frac{P_{21}(r_1)}{r_1}\right)\right]^{-1} ,$$

where

$$A_{100} = (\sqrt{4\pi})\int rP_{10}(r)j_0(kr)\,dr,$$

$$A_{200} = (\sqrt{4\pi})\int rP_{20}(r)j_0(kr)\,dr.$$

The final task is to take the Fourier transform of $v^{\text{exch}}(r)$. For this purpose we represent $v^{\text{exch}}(r)$ as a sum of two functions,

$$v^{\text{exch}}(r) = \sum_i \frac{B_i}{r - r_i^2} + \varphi(r) ,$$

where r_i are the poles of $v^{\text{exch}}(r)$ and $\varphi(r)$ is analytic. Then we have

$$\langle \vec{k}+\vec{q}\,|\,v^{\text{exch}}(r)\,|\,\vec{k}\rangle = v^{(3)}(q,k) = (4/\Omega_0)\{(\pi/2q)$$
$$\times\textstyle\sum_i B_i\cos(qr_i) + \int r^2\varphi(r,k)[\sin(qr)/qr]\,dr\}$$

for $q \neq 0$, and

$$\langle \vec{k}+\vec{q}\,|\,v^{\text{exch}}(r)\,|\,\vec{k}\rangle = v^{(3)}(q,k)$$
$$= \frac{4\pi}{\Omega_0}\left[\sum_i B_i\left(R - \tfrac{1}{2}r_i\ln\left|\frac{r_i+R}{r_i-R}\right|\right) + \int r^2\varphi(r,k)\,dr\right] \quad (\tfrac{4}{3}\pi R^3 = \Omega_0)$$

for $q = 0$.

Figure 1 shows the Fourier components of Slater's exchange and the OPW exchange at 11 and 300 eV. We see that Slater's approximation underestimates the off-diagonal matrix elements, particularly for high values of q. Similar behavior has already been noted by Pendry for Ni.[10] Figure 2 shows the average exchange potential as a function of energy. Again, we note that exchange remains appreciable at high energies. The oscillations in the exchange potential are due to the corresponding oscillations in conduction-electron density which results from the OPW form of the wave function.

Finally, we must account for the presence of other conduction electrons. If one knows their true charge distribution, a set of screening constants can be constructed from its Fourier transforms and used in the plane-wave expansion of the pseudo-wave-function. The difficulty is in obtaining the true charge distribution which should be calculated from the true wave functions. However, we chose to use the distribution obtained directly from the pseudo-wave-functions. Our expression for the screening field obtained in this way is the same to the first order as the expression Harrison[12] calculated from the true wave functions in the small core approximation. The reason is that we kept some higher-order terms arising from the non-Hermitian nature of the pseudopotential in the charge distribution.

In Al the small-core approximation is believed to be well satisfied, and, consequently, the use of pseudo-wave-functions in our screening calculation, rather than the true wave functions, will not lead to any significant errors. In addition, let us note that for Al the smallest wave number used in calculating the Fourier component of the

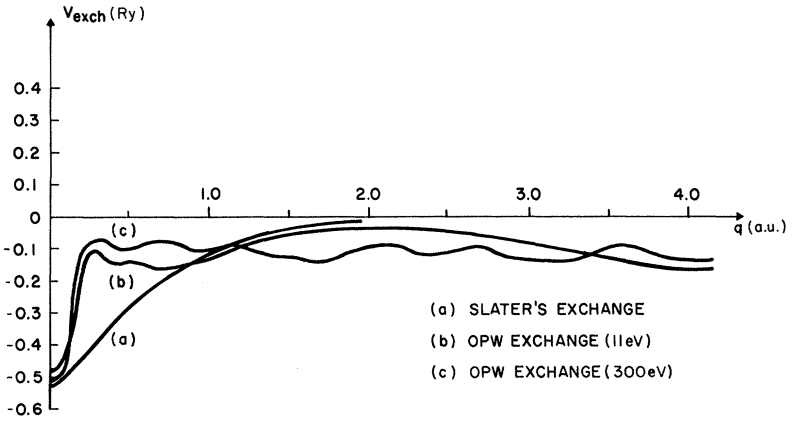

FIG. 1. Fourier components of exchange potential: (a) Slater's exchange; (b) OPW exchange (11 eV); (c) OPW exchange (300 eV).

pseudopotential is $q = 1.425$ a.u., for which the static dielectric function $\epsilon(q)$ is already close to 1 (~ 1.2).

Taking into account the above remarks, we proceed to screen the resulting pseudopotential by dividing its $\vec{k}$-independent part by a static Hartree dielectric function,

$$\epsilon(q) = 1 + \frac{me^2}{2\pi k_F \hbar^2 \eta^2}\left(\frac{1-\eta^2}{2\eta}\ln\left|\frac{1+\eta}{1-\eta}\right| + 1\right) \quad ,$$

where $\eta = q/2k_F$, and by numerically integrating its $\vec{k}$-dependent part over the free-electron Fermi sphere we have

$$\frac{4me^2}{q^2\pi^2\hbar^2}\int_{k<k_F} \frac{\langle \vec{k}+\vec{q}\,|\, W^{\text{rep}} + v^{\text{exch}} \,|\vec{k}\rangle}{|\vec{k}|^2 - |\vec{k}+\vec{q}\,|^2}\, d^3k \quad .$$

Due to the non-Hermitian nature of our pseudopotential, there is an additional term

$$(2/q^2\pi^2)(\textstyle\sum_k \langle \vec{k}+\vec{q}\,|P|\vec{k}\rangle/\epsilon(q)) \quad ,$$

which must be kept to ensure the correct limiting behavior as $q \to 0$.

Figure 3 shows the variation of the off-diagonal matrix elements of the pseudopotential for different energies. We notice that as the energy increases the entire curve is pushed down. For low values of q [such as those corresponding to (111) and (200) reflections] our form factors at $E = E_F$ are in good agreement with Heine-Abarenkov form factors from a model potential.[13] For higher values of q our form factors are somewhat higher, which is due primarily to the OPW exchange. Another interesting feature is that at high values of q, the form factors show similar behavior at high and low energies. It is only in the small-q range where we have significant differences between high- and low-energy form factors. This seems to indicate that for a given orientation between $\vec{k}$ and $\vec{q}$, the $\vec{k}$ dependence of the pseudopotential becomes weaker at high energies.

It is an interesting observation that experimental curves of high- and low-energy form factors for tungsten show the same general behavior as those for Al.[14]

Figure 4 shows the variation of the diagonal matrix elements of the pseudopotential (i.e., the average pseudopotential) with the incident energy. Here again we notice strong dependence on $\vec{k}$ at low energies and possibly asymptotic behavior at high energies.

In the conventional band-structure calculations this term is usually assumed to be constant and is

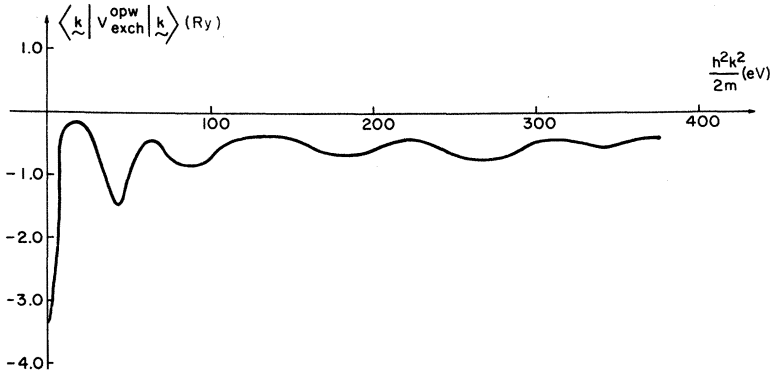

FIG. 2. Average exchange potential versus incident energy.

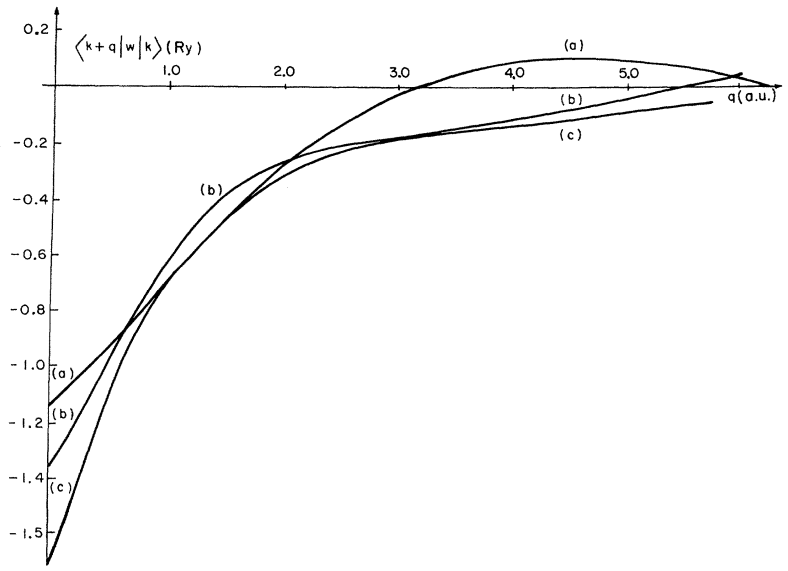

FIG. 3. Off-diagonal matrix elements of the pseudopotential versus incident energy: (a) 57 eV; (b) 147 eV; (c) 518 eV.

taken as the zero reference of energy. This is, of course, quite acceptable since for an infinite system the exact absolute position of the lowest-lying Γ_1 state is poorly defined. Our objective in performing this calculation was to obtain the LEED patterns and compare them with experiment. Neglecting the diagonal $\langle \vec{k}|W|\vec{k}\rangle$ term would necessitate a somewhat arbitrary shift of a theoretical LEED pattern to bring it into an agreement with the experimental one, as has been done in the past. The situation is further complicated by the fact that $\langle \vec{k}|W|\vec{k}\rangle$ depends on energy and consequently the amount of shifting will vary from peak to peak. To avoid this we took considerable pains in calculating the $\langle \vec{k}|W|\vec{k}\rangle$ term and keeping it throughout all calculations. As a result, the absolute position of the experimental LEED peaks was found to be in good agreement with the calculated one.[15]

Figure 5 illustrates the nonlocality of the pseudopotential at 300 eV. Here we plot the matrix elements of the pseudopotential $\langle \vec{k}+\vec{q}|W|\vec{k}\rangle$ versus $|\vec{q}|$ for $k \| \vec{q}$ and $\vec{k} \perp \vec{q}$. We see that the pseudopotential is strongly nonlocal at high energies. Nonlocality becomes somewhat weaker at lower energies. In fact, the entire Fermi surfacr of Al may be obtained with a local pseudopotential using only two matrix elements [for values of q corresponding to (111) and (200) reflections], which indicates that for Al the local approximation holds quite well at low energies.

Using the above-described pseudopotential we calculated the band structure along Δ, Λ, and Σ directions for the fcc lattice. Group theory was used to its fullest advantage, since otherwise the size of a secular determinant becomes prohibitively large. The necessary group theory[16] was incorporated directly into the program, i.e., given two reciprocal-lattice vectors and a representation

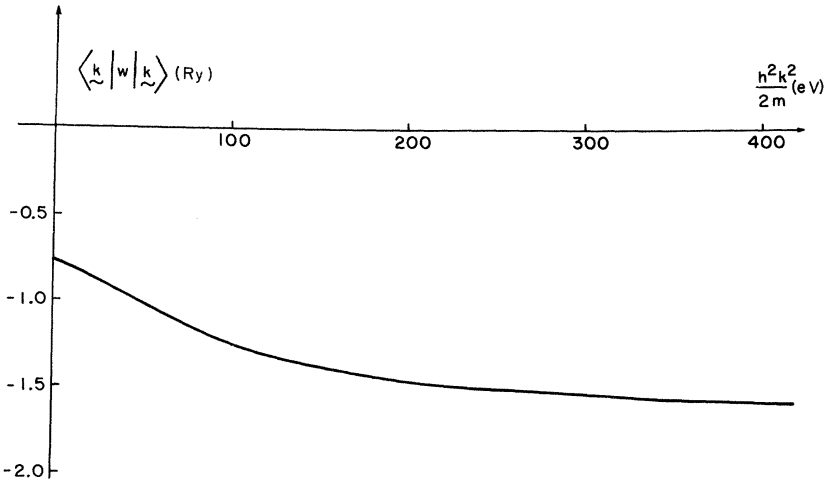

FIG. 4. Diagonal matrix elements of the pseudopotential versus incident energy.

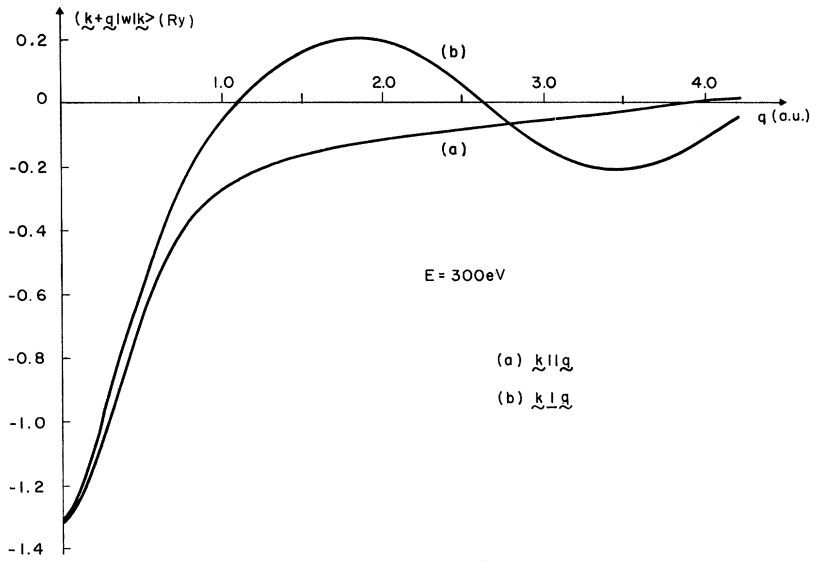

FIG. 5. Nonlocality of the pseudopotential at 300 eV.

label, the program automatically constructs the symmetrized plane waves (SPW) belonging to that irreducible representation and calculates the matrix element between two such SPW, taking into account all possible simplifications allowed by symmetry. In this way, we are able to calculate all of the Γ states with 26 SPW (nearly 600 plane waves), all of the Δ states with 53 SPW's (259 plane waves), all of the χ states with 50 SPW, etc. The largest secular determinant corresponding to 70 SPW was used to calculate the energies of the Σ states. The relative degree of convergence for the lowest-lying states was about 0.02 Ry; at higher energies the convergence necessarily decreases and becomes about 0.2 Ry at the energy of 10 Ry. These estimates were obtained as follows. To check the convergence at lowest energies we calculated the band structure at the Γ point using 4 SPW and 26 SPW, respectively; in going from a 4×4 to a 26×26 determinant the lowest eigenvalue changed by 0.02 Ry. The convergence at the higher energies was checked as follows: Since the Γ point has higher symmetry than any point along the Δ direction, the number of reciprocal-lattice vectors included in the pseudo-wave-function at the Γ point is much larger than the corresponding number for any point along the Δ line (531 plane waves as opposed to 259 plane waves). We used the set of reciprocal-lattice vectors appropriate for the group of Δ to calculate the energies at the Γ point. The largest disagreement found in such calculation did not exceed 0.2 Ry. Thus, we may objectively state that the relative convergence of our band-structure calculation over the entire energy range between 0 and 10 Ry varies from 0.02 to 0.2 Ry. To check the logic of the computer program we calculated the band structure for a particular multidimensional representation using the SPW corresponding to the different columns of that representation. The results were found to be exactly identical.

III. DISCUSSION OF RESULTS AND CONCLUSTIONS

Figures 6, 7, and 8 show the band structure along Δ, Λ, and Σ directions, respectively ([001], [111], and [110] directions); free-electron band structure and the symmetric bands are also shown for comparison. We note that aside from the band gaps the band structure is still very much free-electron-like, which has already been pointed out by Connolly.

Before commenting on the high-energy band structure, let us compare our results with the previously published data of Heine, Segall, Harrison, Snow, and Connolly. Let us consider the band structure along the Δ direction (Fig. 6). For the first band gap $X_1 - X_4'$ we find 0.0171 Ry, while the corresponding results of Heine, Segall, Harrison, and Snow are 0.125, 0.076, 0.108, and 0.082 Ry, respectively. These results emphasize the free-electron-like nature of Al and indicate that Slater's approximation may be adequate in this energy range. Further results on Al are summarized in Table I (where all energies are given relative to the Γ_1 point).

Since we kept the term $\langle \vec{k}|W|\vec{k}\rangle$ on the diagonal we were able to calculate the energy of the lowest-lying Γ_1 point. We found it to be equal to -1.0592 Ry, which is in good agreement with the sum of the Fermi energy level and the work function. As we have already mentioned above, this becomes important in determining the absolute position of

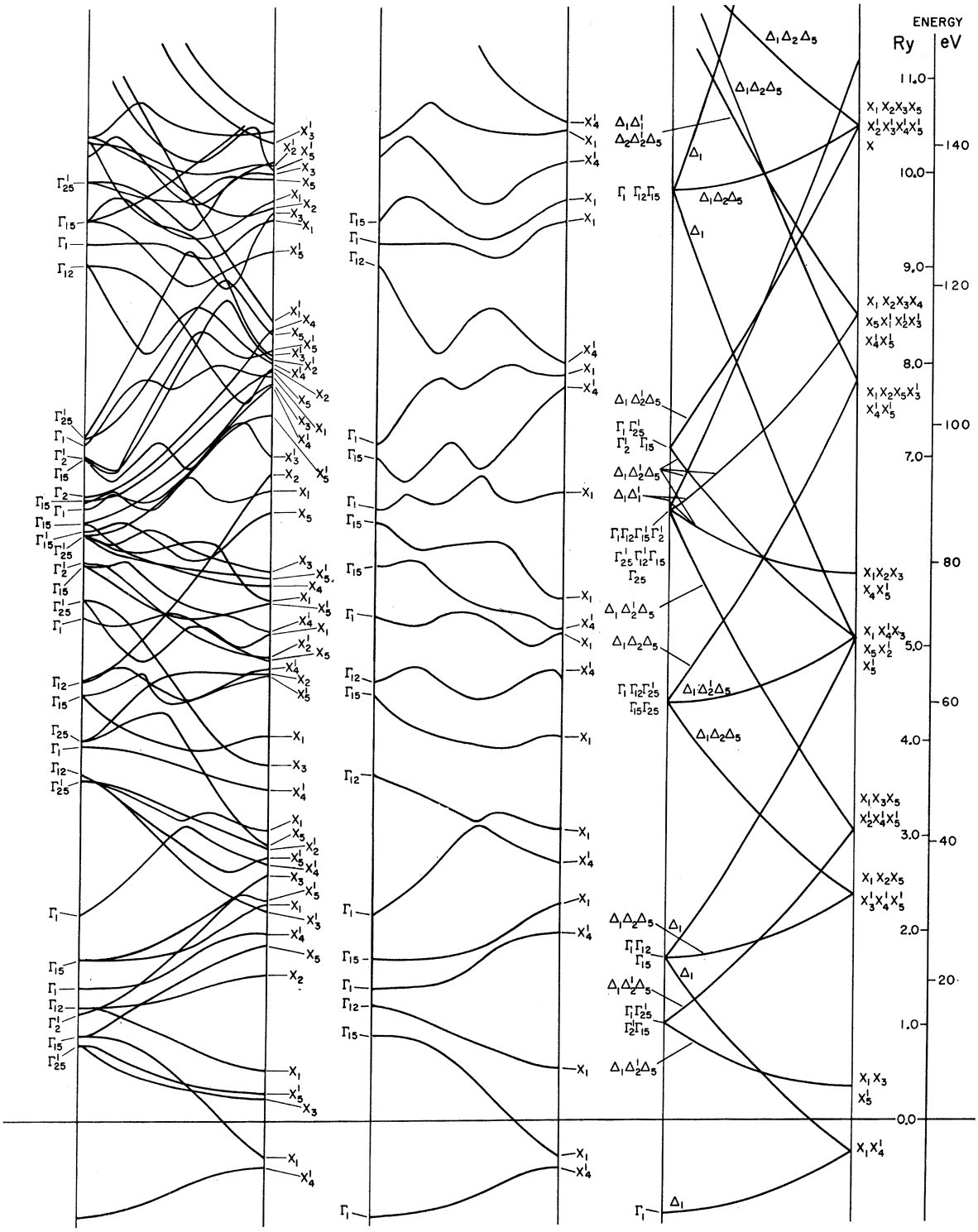

FIG. 6. Band structure along [001] direction: left – complete band structure; center – symmetric bands; right – free-electron bands.

the LEED peaks.

We also feel confident about the results of higher-energy calculations. The only other calculation of high-energy band structure of Al known

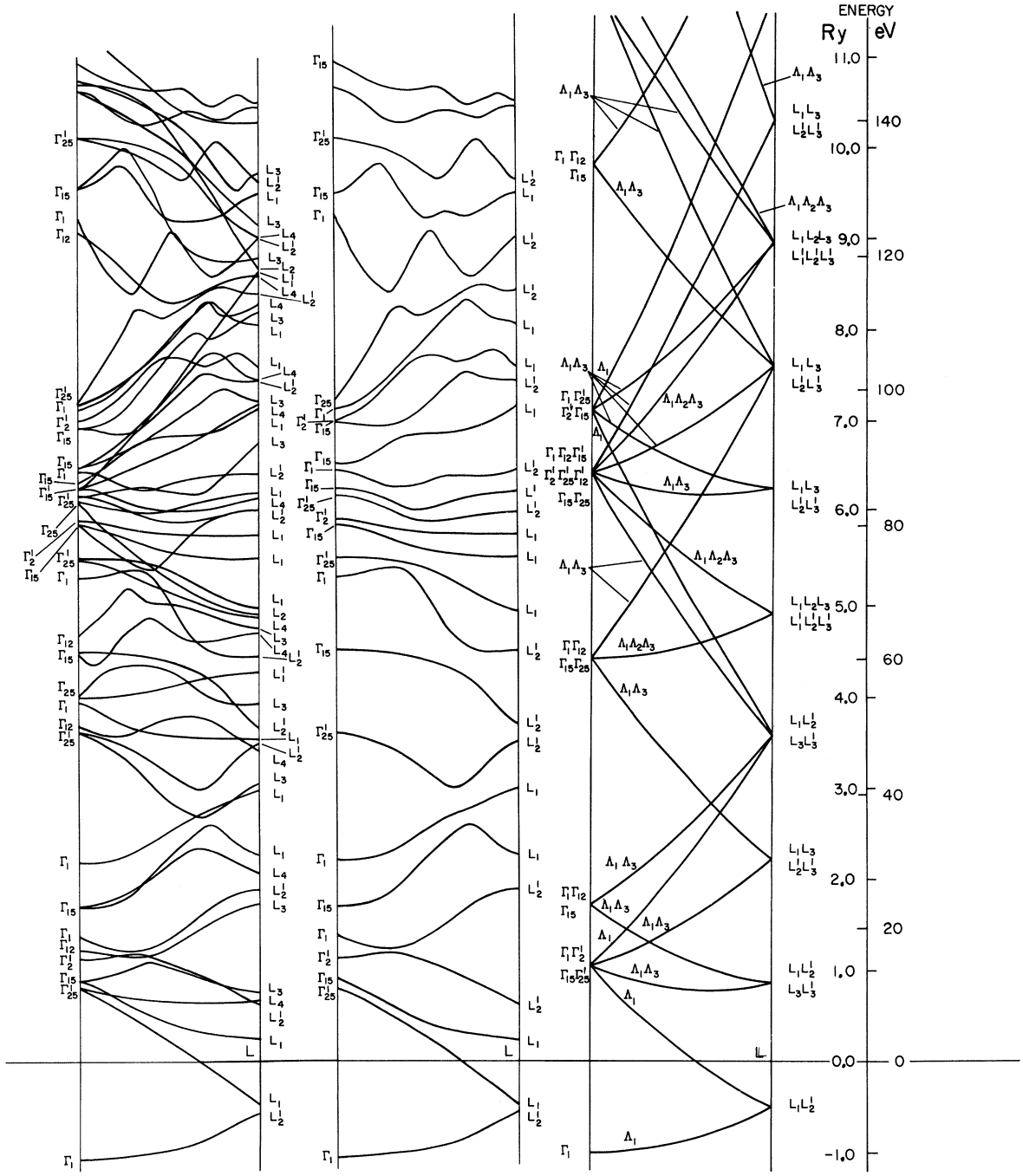

FIG. 7. Band structure along [111] direction: left—complete band structure; center—symmetric bands; right—free-electron bands.

to us was performed by Connolly, who has calculated the band structure up to about 50 V using the APW method. While the general features of both calculations are in qualitative agreement, there are definite discrepancies in the energies .

Finally, let us mention that using the band-structure results presented in this paper we calculated a LEED spectrum for the (001) surface of Al and found good agreement between the experimental and the theoretical results, [15] which also gives a direct experimental confirmation to the calculated band structure.

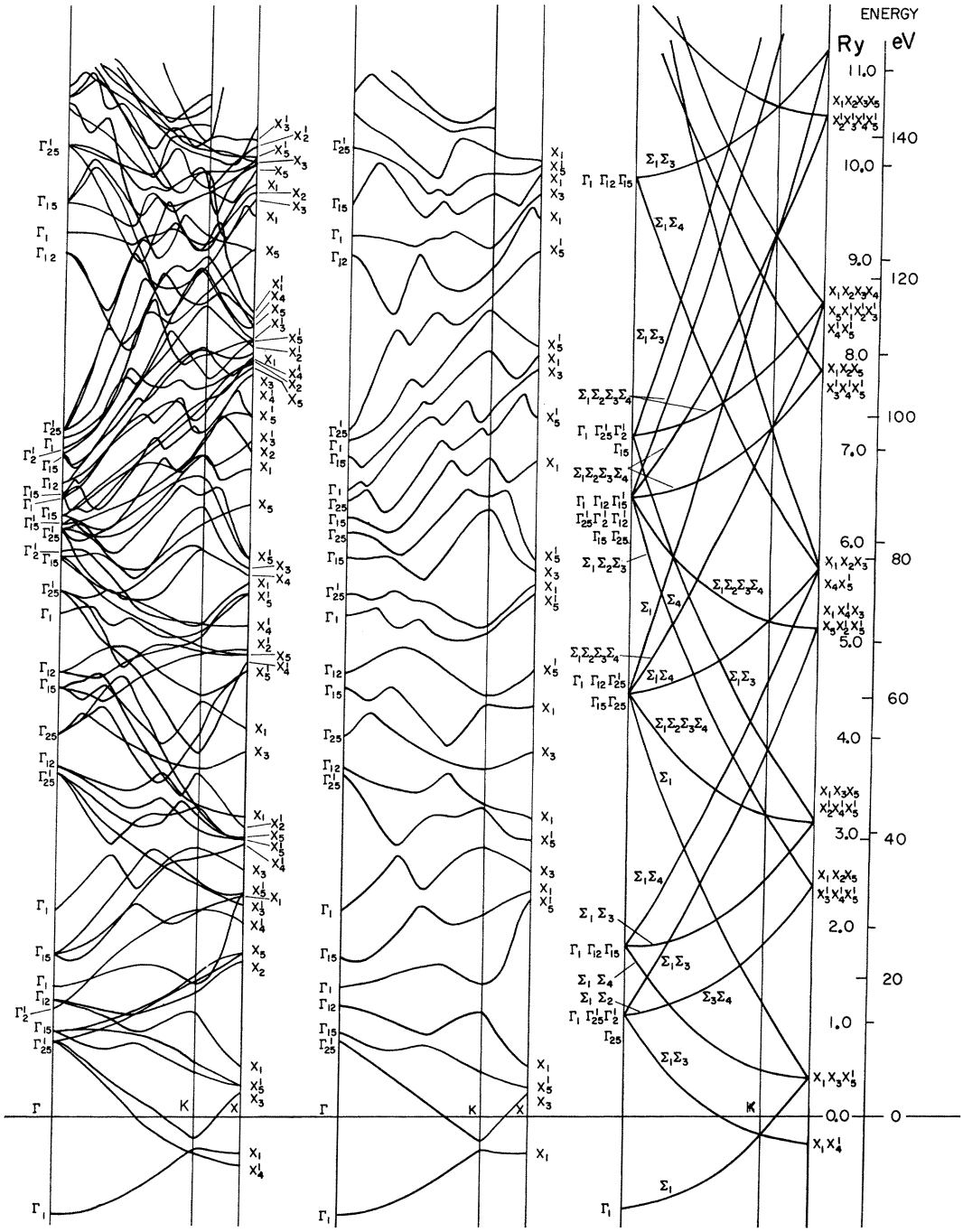

FIG. 8. Band structure along [110] direction: left–complete band structure; center–symmetric bands; right–free-electron bands.

of some of the states. For example, Connolly finds the lowest-lying X_5' point below the X_3 point whereas we find that the opposite is true. In both calculations, however, the separation between these points was found to be about the same. In addition, we see more pronounced deviations from the free-electron band structure in the region of the emerging d bands, such as near the Γ_{12}, Γ_{25}', X_2, X_3, and X_5 states. These discrepancies arise from the fact that both calculations are markedly different not only in the method, but in the construction of potential.

TABLE I. Comparison of energies (in Ry) for states of high symmetry (with respect to $\Gamma_1 = 0$), calculated by different authors. $\langle \vec{k} | W | \vec{k} \rangle_{\Gamma_1} = -1.059$ Ry $= -(E_F + \phi)$, $\phi = 0.31$ Ry.

	Heine (Ref. 1)	Segal (Ref. 6)	Harrison (Refs. 3–5)	Snow (Ref. 7)	Connolly (Ref. 8)	Present paper	Free electron
Γ_1	0.0	0.0	0.0	0.0	0.0	0.0	0.0
X_4'	0.592	0.622	0.585	0.597		0.590	0.677
X_1	0.717	0.698	0.693	0.679		0.700	0.677
X_3					1.20	1.199	
X_5'					1.16	1.259	
L_1		0.512		0.483		0.544	0.501
L_2'		0.483		0.467		0.447	0.501
K_1	0.742	0.723	0.713	0.705		0.699	0.761
K_3	0.699	0.699	0.679	0.673		0.654	0.761
Fermi level			0.84	0.81			0.86

†Work supported by U. S. Air Force Office of Scientific Research, Grant No. AFOSR-1709-69.

*Present address: Laboratorie de Spectrométrie Physique, Grenoble, France.

‡Present address: Materials Research Center, Allied Chemical Corp., Morristown, N. J. 07960.

[1]V. Heine, Proc. Roy. Soc. (London) 240, 354 (1957).

[2]W. A. Harrison, *Pseudopotentials in the Theory of Metals*, (Benjamin, New York, 1966).

[3]W. A. Harrison, Phys. Rev. 116, 555 (1959).

[4]W. A. Harrison, Phys. Rev. 118, 1182 (1960).

[5]W. A. Harrison, Phys. Rev. 136, A1107 (1964).

[6]B. Segall, Phys. Rev. 131, 121 (1963).

[7]E. C. Snow, Phys. Rev. 158, 683 (1967).

[8]J. W. D. Connolly, Bull. Am. Phys. Soc. 14, 359 (1969).

[9]C. Froese-Fisher, *Some Hartree-Fock Results for Atoms Helium to Radon* (British Columbia U. P., British Columbia, Canada, 1968).

[10]J. B. Pendry, J. Phys. C 2, 1215 (1963).

[11]E. A. Kmetko (unpublished).

[12]W. A. Harrison, *Solid State Theory* (McGraw-Hill, New York, 1970).

[13]V. Heine and I. Abarenkov, Phil. Mag. 9, 451 (1964).

[14]H. Taub, Ph. D. thesis, Polytechnic Institute of Brooklyn, 1969 (unpublished).

[15]V. Hoffstein and D. S. Boudreaux, Phys. Rev. Letters 25, 512 (1970).

[16]A. W. Luehrmann, Advan. Phys. 17, 1(1968); see also Ph. D. thesis, University of Chicago, 1967 (unpublished).

PHYSICAL REVIEW B VOLUME 2, NUMBER 8 15 OCTOBER 1970

Screening of a Fixed Charge in the Electron Liquid

A. P. Pathak

Department of Physics, Indian Institute of Technology, Kanpur, India

(Received 16 March 1970)

The static dielectric function given by Kleinman and Langreth has been used to calculate the screening charge density around a fixed foreign charge in an electron liquid for values of r_s which correspond to metallic densities. The results are compared with the earlier results based on the Hubbard approximation, and with those of Singwi and Tosi obtained by a self-consistent procedure.

Since Hubbard[1] proposed approximate methods based on the diagrammatic technique to include the effect of exchange interactions in the RPA expression[2] for the dielectric function in metals, several improvements over his procedure have appeared in the literature.[3-5] The main difficulty with the Hubbard approximation is that it does not account for short-range correlations due to Coulomb repulsion in the electron liquid. Singwi *et al.*[3] used an ansatz to take account of these short-range correlations in an approximate way through a simple physically meaningful function called the pair-distribution function. This ansatz relates the two-particle distribution function $f(1, 1')$ to the one-particle distribution function $f(1)$ and $f(1')$ by

$$f(1, 1') = f(1) f(1') g(\vec{x} - \vec{x}') , \tag{1}$$

where $g(\vec{x} - \vec{x}')$ is the pair-distribution function. Here, 1 and 1′ stand for $\vec{x}$, $\vec{p}$, t and $\vec{x}'$, $\vec{p}'$, t, respectively — the usual position, momentum, and time variables for the two particles. Using Eq. (1) for $f(1, 1')$ in the equation of motion of the one-particle distribution function $f(1)$ in the presence of an external perturbation, Singwi *et al.*[3] obtained an expression for the dielectric function which re-